Experimental study and numerical modelling of a 3 × 100G DP-QPSK superchannel

V.A. Konyshev, A.V. Leonov, O.E. Nanii, A.G. Novikov, P.V. Skvortsov, V.N. Treshchikov, R.R. Ubaydullaev

Abstract. **Crosstalk effects are studied experimentally in a DWDM line with 100G DP-QPSK channels at a frequency convergence of the channels (three channels with a frequency separation of 50, 37.5 and 33 GHz) in the C-band. Spans of 100 km in length are used, with the number of spans varying from one to six. The required optical signal-to-noise ratio ($OSNR_R$) is determined experimentally for a different number of spans, interchannel intervals and input power. We propose a theoretical model based on the numerical modelling that describes the influence of adjacent channels at a strong convergence. The model is calibrated using the obtained experimental data. Based on the proposed model, we calculate the maximal value of the spectral efficiency in systems with a dense arrangement of 100G DP-QPSK channels (~3.2 bit s^{-1} Hz^{-1}).**

Keywords: superchannel, spectral efficiency, crosstalk, channel capacity, Gaussian noise, BER, OSNR.

1. Introduction

Increasing the capacity of fibre-optical communication lines is still an urgent problem. In the case of using the same spectral band, this problem is equivalent to the problem of increasing the spectral efficiency (SE) measured in bit s^{-1} Hz^{-1}. One of the ways to increase the SE is increasing the data transmission rate for each carrier at the expense of using multilevel modulation formats. However, this method considerably reduces the transmission range. In the systems where the signal bandwidth is smaller than that of the optical spectral DWDM channel, one can use alternative methods of SE improvement, e. g., increasing the bit rate, or using superchannels, i. e., a few optical carrier frequencies controlled as an integral whole.

Under laboratory conditions, different configurations of superchannels have been studied [1–4]. For example,

V.A. Konyshev, A.V. Leonov, A.G. Novikov, R.R. Ubaydullaev T8 LLC, office 826, Krasnobogatyrskaya ul. 44/1, 107076 Moscow, Russia; e-mail: leonov.av@t8.ru;
O.E. Nanii T8 LLC, office 826, Krasnobogatyrskaya ul. 44/1, 107076 Moscow, Russia; Faculty of Physics, M.V. Lomonosov Moscow State University, Vorob'evy Gory, 119991 Moscow, Russia;
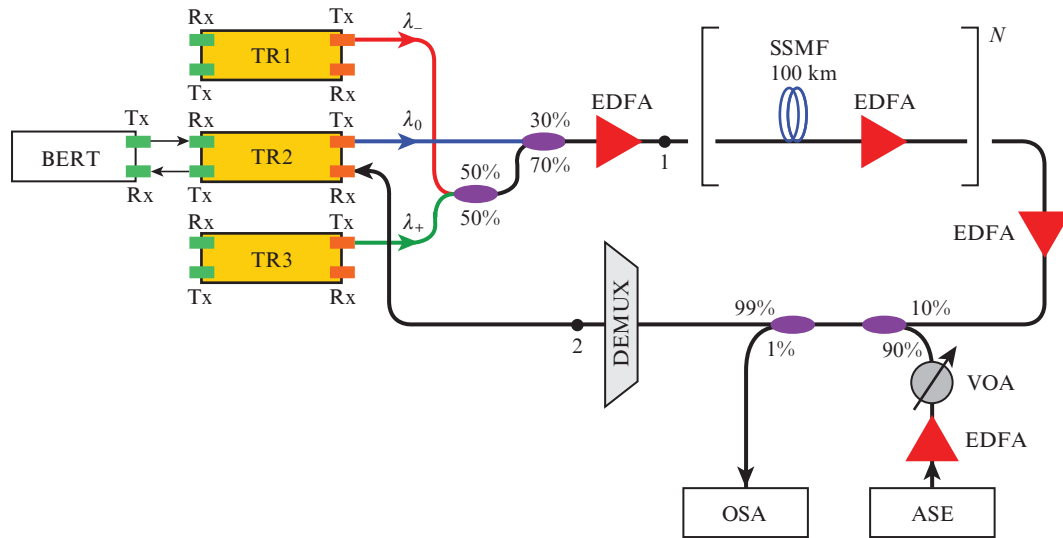**V.N. Treshchikov** T8 LLC, office 826, Krasnobogatyrskaya ul. 44/1, 107076 Moscow, Russia; V.A. Kotel'nikov Institute of Radio Engineering and Electronics (Fryazino Branch), Russian Academy of Sciences, pl. Vvedenskogo 1, 141120 Fryazino, Moscow region, Russia;
P.V. Skvortsov T8 LLC, office 826, Krasnobogatyrskaya ul. 44/1, 107076 Moscow, Russia; Moscow Institute of Physics and Technology (State University), Institutskii per. 9, 141701 Dolgoprudnyi, Moscow region, Russia

Chandrasekhar et al. [1] showed the possibility of organising a superchannel with a capacity of 1.2 Tbit s^{-1}. However, from the practical point of view, the most interesting configurations are those that can be implemented on the basis of the existing network infrastructure (in particular, using 100-GHz grid multiplexers). Also it should be noted that 100 Gbit s^{-1} channels with the DP-QPSK modulation format [5] provide the maximal capacity.

In the present paper, we study the possibility of constructing a 3 × 100 Gbit s^{-1} superchannel in the 100 GHz band (the SE being equal to 3 bit s^{-1} Hz^{-1}). The possibility of reducing the frequency separation between three 100-gigabit channels and the arising penalties are discussed, the theoretical model considering the crosstalk is proposed. The limiting possibilities of the frequency convergence of channels are studied. The proposed 300 Gbit s^{-1} (3 × 100 Gbit s^{-1}) channel in the 100 GHz band provides the SE exceeding by 1.5 times that of the 100 Gbit s^{-1} channel in the 50 GHz band with an insignificant reduction of the working range. Such a superchannel consisting of three wavelengths can be controlled as an integral whole using multiplexers with a 100-GHz frequency plan.

2. Description of the experimental setup

The setup for the experiments aimed at the study of crosstalk effects is schematically shown in Fig. 1. To form three 100 Gbit s^{-1} channels we used three 'Volga' MS100 transponders (T8 LLC) (TR1, TR2 and TR3). A pseudorandom sequence from a BER tester (BERT) was fed to one of the transponders (TR2). Two other transponders produced a linear signal using their pseudorandom sequences. The signals of TR1 and TR3 were combined using a 50/50 coupler and then the mixed signal was coupled to the signal of TR2 using a 70/30 coupler. The obtained signal arrived at the erbium-doped fibre-optical amplifier (EDFA) (booster), using which it was possible to tune the level of the power launched into the line.

The line consisted of 1–6 spans of standard single-mode fibre (SSMF), each being 100 km long. At the end of each span, the signal was amplified by the EDFA. Then the signal passed through the following elements: an EDFA preamplifier providing the amplification of the power before the transponder input, a standard measuring unit and a demultiplexer (DEMUX). The resulting optical signal arrived at the input of one of the transponders, to which the BERT was connected (in our case it was TR2). The chromatic dispersion was compensated for using a digital processor of the transponder.

In the line we used single-type C-band EDFAs possessing a gain at a level of 14–24 dB, an output power up to 200 mW, and an average noise factor of 5 dB. All amplifiers operated in

Figure 1. Schematic of the experimental setup.

the regime of the gain stabilisation. The gain of the booster varied in the course of the experiment. The gains of the EDFAs in the line were chosen to compensate for the attenuation in the spans (19 – 20 dB on average), and the gain of the preamplifier had to provide an optimal signal power at the transponder input (–10 dB).

The measuring unit incorporated a system of noise formation [a source of broadband amplified spontaneous emission (ASE), an optical amplifier (EDFA), and a variable optical

Figure 2. Spectrum of the signal with a channel frequency separation of 33 GHz (a) at the line input (point 1 in Fig. 1) and (b) at the demultiplexer output (point 2 in Fig. 1). The OSA resolution is 0.07 nm.

attenuator (VOA)] and an optical spectrum analyser (OSA). The role of an optical demultiplexer was played by a 40-channel multiplexer with a frequency grid step of 100 GHz.

The radiation frequency f_0 of the central channel of the transponder TR2 did not change in the course of the experiment and amounted to 192.700 THz, which corresponds to the 27th channel of the ITU-T frequency plan (the wavelength 1555.75 nm) [6]. The operating frequencies of the transponders TR1 and TR3 in different experiments amounted to $f_0 \pm 0.050$, $f_0 \pm 0.0375$ and $f_0 \pm 0.033$ THz. The input power in the line was set similar for all three channels. For this purpose, the internal capabilities of the transponders were used (the range of smooth tuning of their output power from – 5 to 0 dBm). To control the power of the channels, the OSA was connected to point 1.

The typical spectrum of the equalised channels (point 1 in Fig. 1) is shown in Fig. 2a. All amplifiers in the line, except the booster, operated in the regime of gain stabilisation to ensure the equality of the powers launched into each span under any conditions of transmission. The signal spectrum at the output from the multiplexer (point 2 in Fig. 1) is shown in Fig. 2b, from which it is seen that the spectrum of the side channels is cut off by the demultiplexer filter (the step of the DEMUX frequency grid amounts to 100 GHz).

3. OSNR and OSNR$_R$ measurement technique

To measure the OSNR we used an optical filter of the spectrum analyser with a width of 1 nm (the maximal value for the used spectrum analyser). This bandwidth of the spectrum analyser filter (1 nm) does not cover all three studied channels completely. Therefore, to recalculate the measured signal power to the real one we introduced the correction coefficient δ ($\delta > 1$), relating the real (P_{real}) and measured (P_{meas}) values of power in the channel:

$$P_{real} = \delta P_{meas}. \tag{1}$$

In the absence of noise (point 1 in Fig. 1) the actual value of the three-channel superchannel power is by three times greater than the single-channel power:
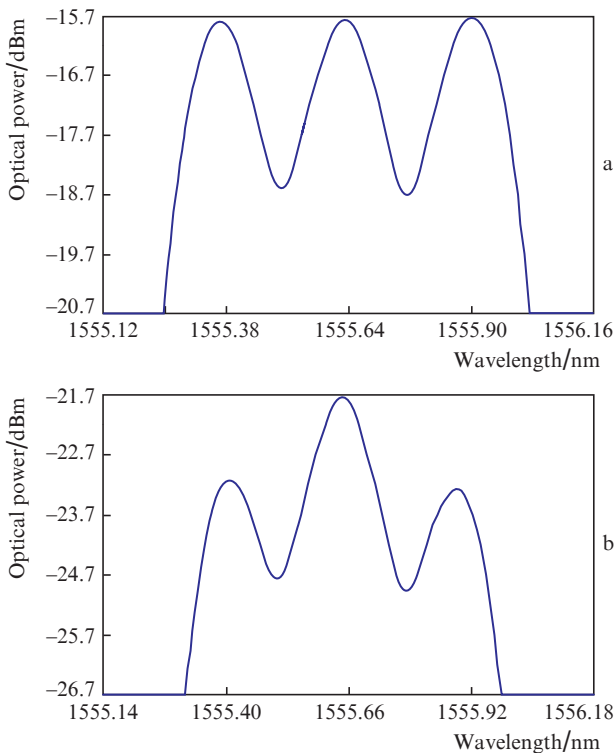
$$P_{\text{real}} = 3P_{\text{ch}}. \tag{2}$$

To calculate δ, the output power P_{ch} of the central channel alone was first measured with the spectrum analyser window 1 nm (the side channels were switched off). Then the power P_{meas} of three channels was measured and the correction coefficient δ was found from relations (1) and (2).

The value of δ is independent of the power in the channels, but depends on the frequency separation between them. It was shown experimentally that for the channel frequency separation of 33 and 37.5 GHz all three channels completely fit into the transmission band of the optical filter with the bandwidth 1 nm, and $\delta = 1$ ($\bar{\delta} = 0$ dB). For the channel frequency separation of 50 GHz, $\delta = 1.21$ ($\bar{\delta} = 10\lg\delta = 0.83$ dB).

With the ASE noise taken into account, the optical (peak) power measured by the spectrum analyser is expressed by the formula

$$P_{\text{meas}} = \frac{3P_{\text{ch}}}{\delta} + P_{\text{ASE}}, \tag{3}$$

where P_{ASE} is the power of the ASE noise in the band $\Delta\lambda = 1$ nm. With Eqn (3) taken into account, the formula for the OSNR in the 0.1 nm band takes the form

$$\text{OSNR}_{0.1} = \frac{P_{\text{ch}}}{P_{\text{ASE}}} \frac{\Delta\lambda}{0.1\,\text{нm}} = \left(\frac{P_{\text{meas}}}{P_{\text{ASE}}} - 1\right)\frac{\delta}{3}10. \tag{4}$$

or in the logarithmic scale

$$\text{osnr}_{0.1} = 10\lg\left(10^{0.1(p_{\text{meas}}-p_{\text{ASE}})} - 1\right) + \bar{\delta} + 5.23\ \text{dB}, \tag{5}$$

where $\text{osnr} = 10\lg(\text{OSNR})$ and $p = 10\lg P$.

To measure the required OSNR (OSNR_{R}) [7] we applied the usual technique of the ASE noise admixing. The power of the noise launched into the line from the optical ASE noise source (see Fig. 1) was smoothly increased by the VOA until the appearance of multiple bit errors and the message about the loss of synchronisation at the BER tester (BERT). After that, the power of the input noise was slightly decreased to restore the line operation, and during 3–5 min the BER testing was executed to make sure that BER does not exceed 10^{-12}. The OSNR was measured using OSA and then recalculated to the bandwidth 0.1 nm according to Eqn (5). The resulting value was accepted as OSNR_{R}.

For the transponder TR2 the level of bit errors BER < 10^{-12} was obtained after the correction of FEC errors, provided that before the FEC procedure the level of BER did not exceed 1.94×10^{-2}. Let us denote by BER_0 this threshold value of BER, exceeding which leads to the line failure.

4. Experimental results and their analysis

Using the experimental setup presented in Fig. 1, we measured the dependences of the required OSNR on the optical signal power launched into the fibre for a different number of spans and different channel frequency separations. The channel frequency separation was taken to be 50, 37.5 and 33 GHz. For the channel frequency separation of 25 GHz it was impossible to achieve the operability of the central channel even for one span and, therefore, the measurements for a greater number of spans were not performed.

With the growth of power P_{ch} launched into the fibre span the required OSNR increases due to the nonlinear distortions of the optical signal. In the linear regime (at small P_{ch}) the results of the measurements did not reveal any dependence of the OSNR_{R} on the number of spans within the limits from one to six. With decreasing channel frequency separation the enhancement of interchannel interference leads to an increase in OSNR_{R}.

The existence of the dependence of OSNR_{R} on the power P_{ch} launched into the span is a manifestation of nonlinear distortions in the received optical signal. It is convenient to describe such distortions as additional noise, additive with respect to the linear ASE noise and the crosstalk [7]:

$$P_{\Sigma} = P_{\text{ASE}} + P_{\text{NLI}} + P_{\text{lin},\chi}, \tag{6}$$

where P_{ASE} is the power of the amplified spontaneous emission noise; $P_{\text{NLI}} = \eta P_{\text{ch}}^3$ is the power of the nonlinear noise; $P_{\text{lin},\chi} = k_{\text{lin},\chi}P_{\text{ch}}$ is the power of the linear crosstalk; and η is the nonlinearity coefficient.

We use the Gaussian noise model (GN-model) [8–12]. In this model, it is assumed that the bit error rate (BER) of the signal depends only on the total noise (the sum of linear and nonlinear noises) and does not depend on the contribution of each type of noise to the total one.

Dividing both sides of Eqn (6) by the power P_{ch} of the signal at the near-end of the span, we obtain

$$\frac{1}{\text{OSNR}_{\text{BER}}} = \frac{1}{\text{OSNR}_{\text{L}}} + \eta P_{\text{ch}}^2 + k_{\text{lin},\chi}, \tag{7}$$

where $\text{OSNR}_{\text{BER}} = P_{\text{ch}}/P_{\Sigma}$ is the ratio of the signal power to the total noise power that determines the BER level in the communication line; and $\text{OSNR}_{\text{L}} = P_{\text{ch}}/P_{\text{ASE}}$ is the ratio of the signal power to the power of ASE noise that can be measured experimentally by means of the optical spectrum analyser OSA. In the linear regime (at a small power) and without the influence of the adjacent channels $\text{OSNR}_{\text{BER}} = \text{OSNR}_{\text{L}}$, and so in this case one can measure the dependence of BER on OSNR_{BER} (the calibration curve). In the nonlinear regime, it is impossible to measure OSNR_{BER} directly, but it is possible to calculate the BER level using the calibration curve.

The condition of line operability has the form [13]

$$\text{OSNR}_{\text{BER}} > \text{OSNR}_{\text{BTB}}, \tag{8}$$

or

$$\frac{1}{\text{OSNR}_{\text{L}}} < \frac{1}{\text{OSNR}_{\text{BTB}}} - \eta P_{\text{ch}}^2 - k_{\text{lin},\chi}. \tag{9}$$

Here the OSNR_{BTB} (back-to-back OSNR, the required OSNR in a short line) is the constant, which is a characteristic of the transponder. Thus the critical OSNR, at which the line is still workable, is expressed by the formula

$$\frac{1}{\text{OSNR}_{\text{R}}} = \frac{1}{\text{OSNR}_{\text{BTB}}} - \eta P_{\text{ch}}^2 - k_{\text{lin},\chi}. \tag{10}$$

For the transponder TR2 the constant OSNR_{BTB} was found experimentally using the calibration curve, namely, $\text{osnr}_{\text{BTB}} = 11.93$ dB, which corresponds to $1/\text{OSNR}_{\text{BTB}} = 6.41\times10^{-2}$.

From relation (10) it follows that in order to calculate the linear and nonlinear coefficients it is reasonable to plot the

dependence of the inverse required OSNR on the squared power. Such dependences for the central channel with the number of spans from 1 to 6 and for the interchannel frequency separation of 50, 37.5 and 33 GHz are presented in Figs 3a, 3b and 3c, respectively.

The most important result is that $k_{\mathrm{lin},\chi}$ is a function of the interchannel interval and does not depend either on the number of spans (the crossing with the coordinate axis occurs nearly at the same point for each interchannel frequency spac-

ing), or on the launched power (otherwise the plots would not be linear). This confirms our hypothesis that the effect of the adjacent channels is well described by the model of linear additive noise.

Thus, the experiment confirms the linear character of the action of adjacent channels on the studied one. Three different values of $\mathrm{OSNR_R}$ were obtained corresponding to three different interchannel intervals in the linear operation regime of the line, which will be used below (Section 5) to calibrate the numerical model.

5. Model of the effect of adjacent channels

To study the intercation of channels at their frequency convergence, a computational model in the MATLAB environment was developed using the model of additive white Gaussian noise (AWGN) with the crosstalk taken into account. The model was calibrated using the experimental data as shown below.

Considering the QPSK modulation format for a single channel, one can write the relation

$$y(n) = x(n) + w(n), \; n = 1, 2, ..., L, \tag{11}$$

where $y(n)$ is the received signal; $x(n)$ is the transmitted QPSK symbol; $w(n)$ is the complex-valued Gaussian process with a zero mean value and variance $2\sigma^2$; and L is the number of the observed symbols. Assuming ideal synchronisation (when the necessary readouts are made in the central part of the symbols), the received and transmitted signals can be decomposed into the in-phase (I) and quadrature (Q) components

$$y_{\mathrm{I}}(n) = x_{\mathrm{I}}(n) + w_{\mathrm{I}}(n), \tag{12}$$

$$y_{\mathrm{Q}}(n) = x_{\mathrm{Q}}(n) + w_{\mathrm{Q}}(n). \tag{13}$$

The quantities $x_{\mathrm{I}}(n)$ and $x_{\mathrm{Q}}(n)$ are independent and similarly distributed; they take the values $\{a, -a\}$. The quantities $w_{\mathrm{I}}(n)$ and $w_{\mathrm{Q}}(n)$ correspond to the Gaussian processes with the variances $\sigma_{\mathrm{I}}^2 = \sigma_{\mathrm{Q}}^2 = \sigma^2$.
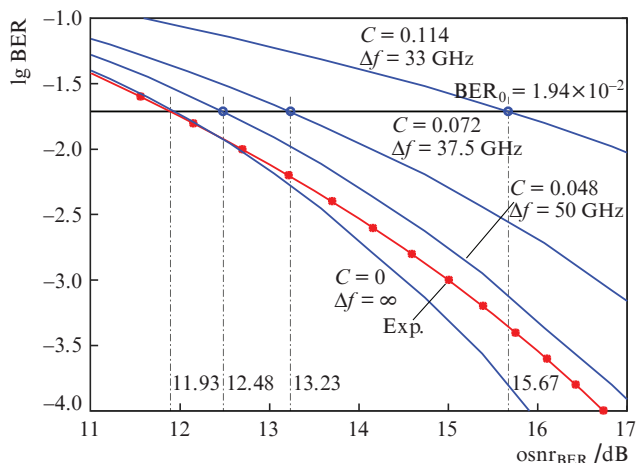
The signal-to-noise ratio for the received signal is defined as

$$\mathrm{SNR} = \frac{S}{N} = \frac{x_{\mathrm{I}}^2 + x_{\mathrm{Q}}^2}{E(w_{\mathrm{I}}^2 + w_{\mathrm{Q}}^2)} = \frac{a^2}{\sigma^2}. \tag{14}$$

Using Eqns (12) and (13) for a sufficiently high number of transmitted signals it was possible to find the calculated BER for each given σ, and the SNR corresponding to this σ was calculated using Eqn (14). Thus, we found the calculated dependence of BER on SNR in the case of a single channel (the sequence of 10^7 symbols was used). By comparing this dependence with the calibration curve (BER versus OSNR for a single channel in a short line, the curve 'Exp.' in Fig. 4) we found the proportionality ratio $B_{\mathrm{el}}/B_{\mathrm{opt}}$ between the calculated SNR value and the experimental OSNR value ($\mathrm{SNR} \times B_{\mathrm{el}} = \mathrm{OSNR} \times B_{\mathrm{opt}}$). The discrepancy between the calculated dependence for a single channel and the experimental calibration curve in the region of high OSNR can be explained by the influence of transponder internal noises that were not taken into account in the numerical model (11)–(13).

To take the effect of the adjacent channels into account, the basic model (11)–(13) was completed by the additional
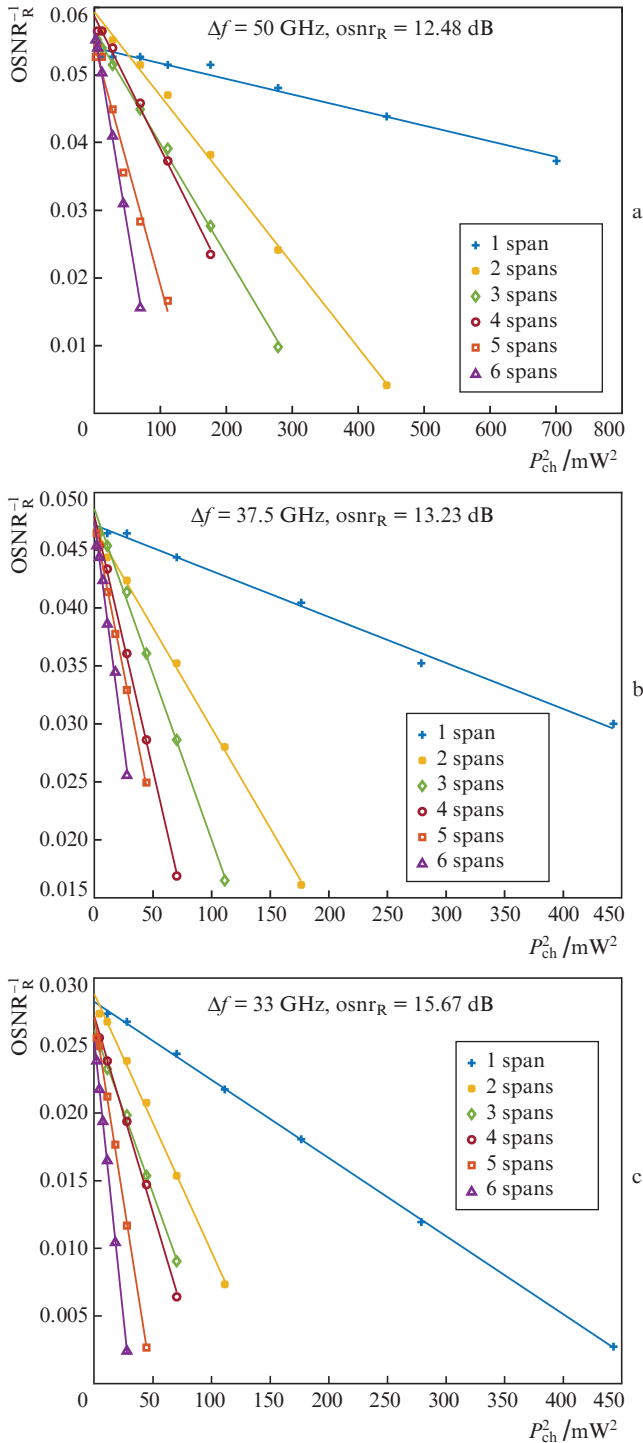
Figure 3. Dependences of the inverse required OSNR on the squared input power at different frequency separations between the channels.

Figure 4. Dependence of the BER level on the optical signal-to-noise ratio for different values of the coefficient C, as well as the experimental calibration curve (Exp.).

term describing the action of the adjacent channels on the received signal. We assume that this influence is described by the real-valued function $C(\Delta f)$ depending only on the frequency separation. Thus, in the simplest model considering the influence of the adjacent channels relation (11) for the received signal is modified as

$$y(n) = x(n) + w(n) + C(\Delta f)[x^-(n) + x^+(n)], \ n = 1,2,...,L, \ (15)$$

where

$$y(n) \equiv [y_I(n) + jy_Q(n)]e^{j\omega t_n},$$

$$x(n) \equiv [x_I(n) + jx_Q(n)]e^{j\omega t_n} = e^{j\varphi_n} e^{j\omega t_n},$$

$$x^-(n) \equiv [x_I^-(n) + jx_Q^-(n)]e^{j\omega^- t_n} = e^{j\varphi_n^-} e^{j\omega^- t_n},$$

$$x^+(n) \equiv [x_I^+(n) + jx_Q^+(n)]e^{j\omega^+ t_n} = e^{j\varphi_n^+} e^{j\omega^+ t_n}.$$

Here φ_n, φ_n^-, φ_n^+ are independent random quantities, taking the values $\pi/4$; $3\pi/4$; $5\pi/4$; $7\pi/4$. In our model, relations (15) for the quadrature components have the form

$$y_I(n) = x_I(n) + w_I(n) + C(\Delta f)\{[x_I^+(n) + x_I^-(n)]\cos(2\pi\Delta f t_n)$$

$$+ [x_Q^-(n) - x_Q^+(n)]\sin(2\pi\Delta f t_n)\}, \quad (16)$$

$$y_Q(n) = x_Q(n) + w_Q(n) \ C(\Delta f)\{[x_I^+(n) - x_I^-(n)]\sin(2\pi\Delta f t_n)$$

$$+ [x_Q^+(n) + x_Q^-(n)]\cos(2\pi\Delta f t_n)\}, \quad (17)$$

where $t_n = n\tau$, and we assume that $\omega^+ - \omega = \omega - \omega^- = 2\pi\Delta f$ (ω is the frequency of the central channel, and Δf is the interchannel frequency separation). Without loss of generality, it is convenient to proceed from the random phases φ_n, φ_n^-, φ_n^+ to the random values of quadratures $x_I(n)$, $x_Q(n)$, $x_I^-(n)$, $x_Q^-(n)$, $x_I^+(n)$, $x_Q^+(n)$, each of them capable of taking the values $\{-a,a\}$ (the separation between the symbols being equal to $2a$).

For small powers of the input signal, BER is a function of the ASE noise (recalculated to the σ/a ratio) and the interchannel frequency sepatation Δf.

Using the proportionality ratio B_{el}/B_{opt} found above, for different values of C the calculated dependences of BER on OSNR were determined for the central channel under the condition of interaction of two adjacent channels (a sequence of 10^7 symbols was used). By means of the trial-and-error method, we found three values of C, at which the values of $OSNR_R$ earlier determined experimentally for three different interchannel frequency separations (Fig. 4) correspond to the threshold level of bit errors BER_0. The values of C for three different Δf are presented in Table 1.

Table 1. Values of C for different interchannel intervals.

Δf /GHz	$osnr_R$ /dB	C
∞	11.93	0
50	12.48	0.048
37.5	13.23	0.072
33	15.67	0.114

Let us search the approximating function in the form $C(\Delta f) = a_1/(\Delta f - a_2)^{a_3}$. Solving the system of three equations for three different C ($\Delta f = 50$, 37.5 and 33 GHz), the following values of the approximating function parameters were found:

$$a_1 = 0.143, \ a_2 = 31.15 \ \text{ГГц}, \ a_3 = 0.373.$$

Thus, in the proposed theoretical model the minimal separation between the channels is limited by the value 31.15 GHz, and the corresponding spectral efficiency amounts to ~ 3.2 bit s^{-1} Hz^{-1}.

6. Conclusions

The possibility of frequency convergence of 100 Gbit s^{-1} channels is demonstrated experimentally for data transmission over three channels in a standard 100 GHz multiplexer window (the spectral efficiency of such superchannel amounts to 3 bit s^{-1} Hz^{-1}). The theoretical model is constructed based on the assumption of a linear effect of adjacent channels on the studied channel. The model is calibrated using the obtained experimental data. Using the developed model it is shown that the maximal spectral efficiency attainable by the convergence of channels is limited by the value 3.2 bit s^{-1} Hz^{-1}.

It is worth noting that the nearest future of high-speed communication system development consists in the use of the 64 Gbaud symbol rate and the modulation formats up to DP-64QAM, which allows the transmission of up to 600 Gbit s^{-1} using one carrier in the 100 GHz band. However, in this case an essential fall of the transmission range occurs. Thus, e. g., the $osnr_R$ for the 400 Gbit s^{-1} system in the 100-GHz window using one carrier (DP-16QAM, 64 Gbaud) is estimated to be 20 dB [14]. The version of superchannel organisation proposed in the present paper presents an alternative way to increase the spectral efficiency in the 100 GHz grid, providing the $osnr_R$ less than 16 dB.

References

1. Chandrasekhar S., Liu X., Zhu B., Peckham D. *Proc. Europ. Conf. Opt. Commun. (ECOC'2009)* (Vienna, Austria, 2009) pp 1–2.
2. Zeng T. *Opt. Express*, **21** (12), 14799 (2013).
3. Souza A.L. et al. *J. Opt. Commun. and Networking*, **8** (7), A152 (2016).

4. Maher R., Alvarado A., Lavery D., Bayvel P. *Sci. Rep.*, **6**, 110 (2016).
5. Konyshev V.A., Leonov A.V., Naniy O.E., Treshchikov V.N., Ubaydullaev R.R. *Pervaya Milya*, **6**, 40 (2015).
6. ITU-T Recommendation G.694.1. Spectral Grids for WDM Application: DWDM Frequency Grid (2002).
7. Konyshev V.A., Leonov A.V., Nanii O.E., Treshchikov V.N., Ubaydullaev R.R. *Opt. Commun.*, **355**, 279 (2015).
8. Splett A., Kurtzke C., Petermann K. *Proc. ECOC* (Montreaux, Switzerland, 1993) Vol. 2, pp 41–44.
9. Poggiolini P., Carena A., Curri V., Bosco G., Forghieri F. *IEEE Photon. Technol. Lett.*, **23** (11), 742 (2011).
10. Carena A., Curri V., Bosco G., Poggiolini P., Forghieri F. *J. Lightwave Technol.*, **30** (10), 1524 (2012).
11. Poggiolini P. *J. Lightwave Technol.*, **30** (24), 3857 (2012).
12. Poggiolini P., Bosco G., Carena A., Curri V., Jiang Y., Forghieri F. *J. Lightwave Technol.*, **32** (4), 694 (2014).
13. Konyshev V.A., Leonov A.V., Naniy O.E., Novikov A.G., Treshchikov V.N., Ubaydullaev R.R. *Quantum Electron.*, **46** (12), 1121 (2016) [*Kvantovaya Elektron.*, **46** (12), 1121 (2016)].
14. Reis J.D. (Ed.) *400G White Paper. Technology Options for 400G Implementation (OIF-Tech-Options-400G-01.0)* (Fremoont, Cal., USA, 2015).